

QADM-Net: Multi-Level Quality-Adaptive Dynamic Network for Reliable Multimodal Classification

Shu Shen, C. L. Philip Chen, Tong Zhang

Abstract

Multimodal machine learning has achieved remarkable progress in many scenarios, but its reliability is undermined by varying sample quality. In this paper, we find that current multimodal classification methods lack dynamic networks for sample-specific depth and parameters to achieve reliable inference. To this end, a novel framework for multimodal reliable classification termed Multi-Level Quality-Adaptive Dynamic Multimodal Network (QADM-Net) is proposed. QADM-Net first adopts a novel approach based on noise-free prototypes and a classifier-free design to reliably estimate the quality of each sample at both modality and feature levels. It then achieves sample-specific network depth via the *Global Confidence Normalized Depth (GCND)* mechanism. By normalizing depth across modalities and samples, *GCND* effectively mitigates the impact of challenging modality inputs on dynamic depth reliability. Furthermore, QADM-Net provides sample-adaptive network parameters via the *Layer-wise Greedy Parameter (LGP)* mechanism driven by feature-level quality. The cross-modality layer-wise greedy strategy in *LGP* designs a reliable parameter prediction paradigm for multimodal networks with variable depths for the first time. Experiments conducted on four datasets demonstrate that QADM-Net significantly outperforms state-of-the-art methods in classification performance and reliability, exhibiting strong adaptability to data with diverse quality.

1 Introduction

In recent years, the accessibility of multimodal data has significantly enhanced prediction across various application scenarios [Dou *et al.*, 2022; Li *et al.*, 2022; Sun *et al.*, 2022; Elizalde *et al.*, 2023]. However, multimodal samples often display complex quality variations due to inherent differences in informativeness across modalities and the noise introduced by varying sensor conditions or environmental factors [Zhang *et al.*, 2024]. This phenomenon poses substantial challenges for reliable prediction, especially in safety-critical domains such as computer-aided diagnosis and au-

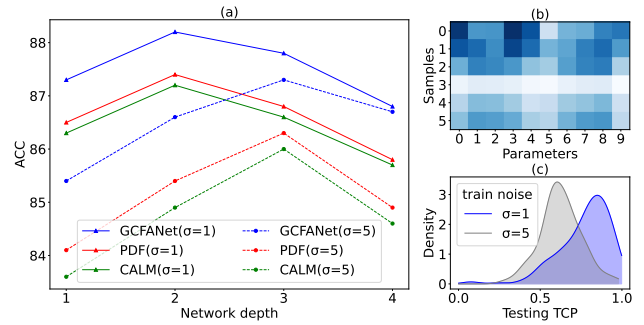


Figure 1: Empirical studies under varying data quality. We simulate data quality degradation by adding Gaussian noise, with σ representing the noise intensity. (a) The classification accuracy corresponds to different network depths on the noisy modality with varying noise intensity. The results of three state-of-the-art reliable multimodal classification methods including CALM [Zhou *et al.*, 2023], GCFANet [Zheng *et al.*, 2024], and PDF [Cao *et al.*, 2024] are shown. (b) Visualization of the model parameters required to map samples with different features to their corresponding class centers. (c) The confidence estimation results on the *same test samples* provided by TCP [Han *et al.*, 2022] as a representative example after *training on data with different noise intensities*. **More details are included in the supplementary material.**

tonomous driving [Feng *et al.*, 2018; Nair *et al.*, 2020; Han *et al.*, 2022; Zhou *et al.*, 2023]. Consequently, extensive research [Geng *et al.*, 2021; Han *et al.*, 2022; Zou *et al.*, 2023; Zheng *et al.*, 2023; Tellamekala *et al.*, 2023; Zhou *et al.*, 2023; Zhang *et al.*, 2023; Zheng *et al.*, 2024; Cao *et al.*, 2024] has focused on developing reliable multimodal classification methods to handle data with varying quality. These methods evaluate the quality of samples and remove uninformative features in low-quality data, thus enhancing the reliability of learning results.

However, empirical studies reveal several limitations of current reliable multimodal classification methods when dealing with data of varying quality. **(1) Lack of network dynamics.** We analyze the quality variation of multimodal samples at both the modality and feature levels. At the modality level, the optimal network depth grows as the modality quality declines (see the two curves for the same model in Figure 1 (a)). At the feature level, mapping feature vectors with

different feature values to the most reliable representations (i.e., class centers) requires distinct network parameters, as shown in Figure 1 (b). Unfortunately, existing methods are static networks with fixed network depth and parameters. (2) **Lack of reliable confidence estimation.** These methods typically produce confidence estimation results that are sensitive to training noise, as shown in Figure 1 (c) and 5, leading to decreased reliability. Moreover, they cannot simultaneously perform multi-level (the modality and feature levels) quality estimation of a sample. Thus, we pose two key questions: (1) *How can we design a robust multi-level quality estimation method to support reliable network adjustments?* (2) *How can we adjust the network’s depth and parameters to ensure reliability for a given multimodal sample?*

This paper addresses the above questions by proposing Multi-Level Quality-Adaptive Dynamic Multimodal Network (QADM-Net), a novel framework for reliable multimodal classification. QADM-Net first adopts *noise-free prototype confidence estimation (NFCE)* to reliably assess sample quality at both the modality and feature levels. Then, QADM-Net sequentially employs the *Global Confidence Normalized Depth (GCND)* and *Layer-wise Greedy Parameter (LGP)* mechanisms to adjust its depth and parameters based on modality- and feature-level qualities of the sample, respectively. Unlike existing confidence estimation methods, *NFCE* derives class probability from pre-optimized noise-free prototypes (i.e., noise-removed class centers) and a classifier-free design, instead of using network structures or classifiers. This design enables multi-level and reliable quality estimation by avoiding overfitting to training noise in the network structure and classifier. The *GCND* mechanism maps sample modality quality to network depth. Notably, it reduces the impact of extremely difficult modality inputs by normalizing depths across modalities of all samples, thereby enhancing the reliability of dynamic depth. The *LGP* mechanism further performs cross-modality parameters prediction aiming to maximize feature-level quality enhancement at each layer. This mechanism introduces a reliable parameter prediction framework across multimodal networks of varying depths for the first time.

The contributions of this paper can be summarized as:

- We delve into reliable multimodal learning from a novel perspective by portraying the dynamics of network depth and parameters to accommodate quality variations of different data at the modality and feature levels.
- The proposed confidence estimation method based on noise-free prototypes and classifier-free design surpasses existing methods in avoiding noise overfitting and achieving multi-level quality assessment.
- The two proposed dynamic mechanisms with cross-modality depth normalization and parameters prediction, design a new paradigm that endows dynamic networks with multimodal reliability for the first time.
- The proposed QADM-Net outperforms state-of-the-art reliable multimodal learning methods in multiple benchmarks by a large margin and exhibits strong adaptability to data with various qualities.

Comparison with existing works. We discuss the key differences between QADM-Net and other works. (1) **Reliable multimodal classification methods:** existing methods based on static networks, while QADM-Net possesses network dynamics and adaptability towards different input samples. (2) **Dynamic neural networks (DNNs):** Our method endows DNNs with multimodal reliability for the first time. Most DNNs, except for DynMM [Xue and Marculescu, 2023], are unimodal and cannot be extended to multimodal scenarios. All DNNs, including DynMM, commonly lack reliability in both confidence estimation and dynamic mechanism design. QADM-Net complements these methods by offering reliable multi-level confidence estimation and robust dynamic mechanisms based on sample’s quality and cross-modality relationships. (3) **Confidence estimation methods:** The proposed *NFCE* is orthogonal to existing confidence estimation methods, i.e., *NFCE* can be used to improve the reliability of these methods and achieve multi-level quality estimation.

2 Related Works

Due to space limitations, this section highlights only a selection of related works. **For a more comprehensive overview, please refer to the supplementary material.**

2.1 Reliable Multimodal Classification

Many studies have developed quality-aware methods to provide reliable multimodal classification results from low-quality multimodal data. Han et al. [Han et al., 2022] modeled informativeness at the feature and modality levels, achieving trustworthy multi-modal feature fusion. Zhang et al. [Zhang et al., 2023], Cao et al. [Cao et al., 2024] achieved more robust and generalized multimodal fusion by dynamically assigning weights to each modality based on uncertainty estimation. Zheng et al. [Zheng et al., 2023] achieved trustworthy multimodal classification via integrating feature and label-level confidence.

2.2 Confidence Estimation

In reliable multimodal classification methods, confidence estimation measures the quality of input features, serving as a necessary foundation for the model’s reliability. Some methods use Maximum-Class Probability (MCP) for confidence estimation [Zou et al., 2023], while others adopt True Class Probability (TCP) [Han et al., 2022; Cao et al., 2024], and some rely on energy scores [Zhang et al., 2023]. These methods commonly estimate confidence based on the class probability of input obtained by classifiers or network structures.

2.3 Dynamic Neural Network

Designing dynamic mechanisms is a promising approach to promoting neural networks’ accuracy and computational efficiency [Veit and Belongie, 2018; Hua et al., 2019; Su et al., 2019; Han et al., 2021]. [Huang et al., 2017] utilized early exit to enable efficient inference for samples. Lin et al. [Lin et al., 2023] achieved accuracy-speed trade-offs by applying different network routines to each sample. Xue et al. [Xue and Marculescu, 2023] introduced DynMM, a dynamic multimodal fusion approach that reduces computational costs while maintaining accuracy.

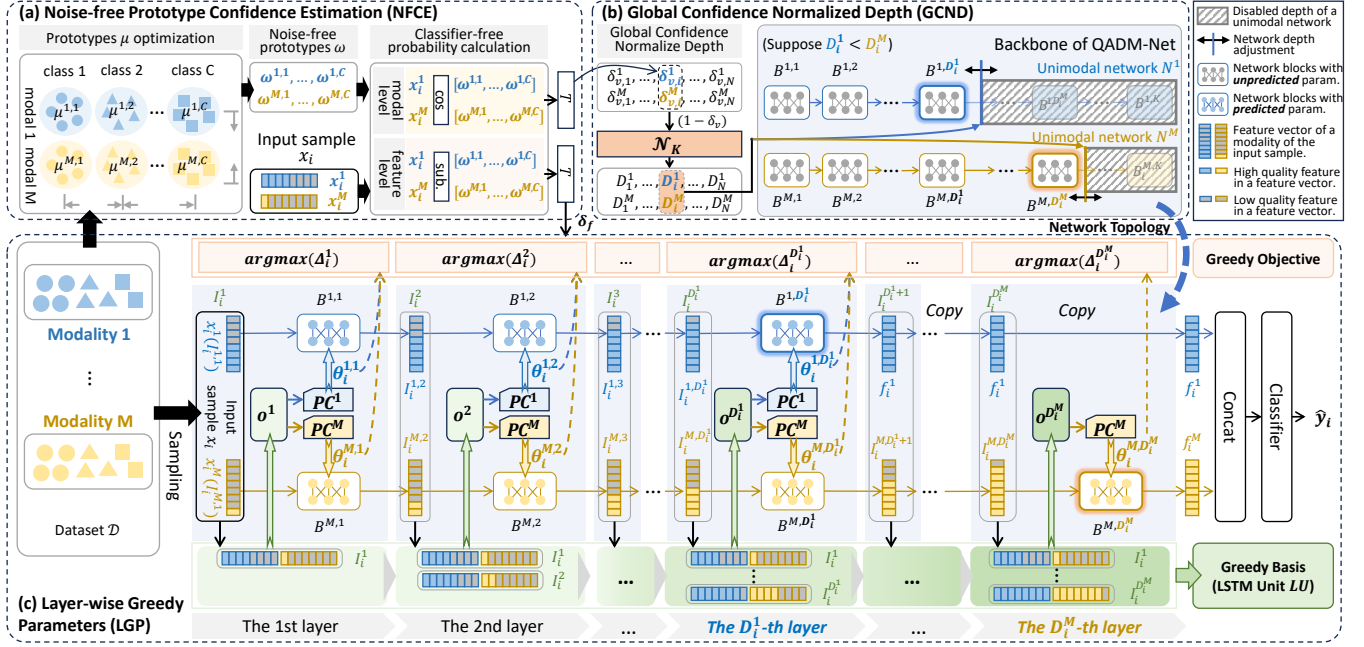


Figure 2: The framework of the proposed QADM-Net. For an input sample x_i from dataset \mathcal{D} : (a) the modality-level and feature-level quality of x_i is estimated via *Noise-free Prototype Confidence Estimation (NFCE)*. (b) The reliable depth of QADM-Net for x_i is adjusted by *Global Confidence Normalized Depth (GCND)* based on modality-level quality. (c) The reliable parameters of QADM-Net for x_i are adjusted by *Layer-wise Greedy Parameter (LGP)* based on feature-level quality.

3 Proposed QADM-Net

In this section, we provide a detailed illustration of the proposed QADM-Net. Given a multimodal dataset $\mathcal{D} = \{(x_i, y_i)\}_{i=1}^N$ containing N samples with M modalities belonging to C classes. Multimodal classification methods aim to learn a neural network that maps every input sample $x_i = \{x_i^m \in \mathbb{R}^{d^m}\}_{m=1}^M$ to its corresponding class label $y_i \in \mathbb{R}^C$, where d^m is the dimension of the m -th modality. In this work, we propose QADM-Net to provide reliable classification result \hat{y}_i for input sample x_i via sample-adaptive network depth and parameters.

3.1 Backbone of QADM-Net

We first introduce the hierarchical backbone structure of QADM-Net. QADM-Net consists of M unimodal networks $N^m (m \in [1, M])$. Each N^m comprises \mathbf{D}^m network blocks $B^{m,t} (t \in [1, \mathbf{D}^m])$. Each network block $B^{m,t}$ contains a fully connected layer with parameters $\theta^{m,t} = [W^{m,t}, b^{m,t}]$, where $W^{m,t}, b^{m,t}$ refers to weight and bias.

Given an input sample $x_i = \{x_i^m\}_{m=1}^M$, the depth \mathbf{D}^m of each unimodal network is adjusted to \mathbf{D}_i^m , and all network block parameters $\theta^{m,t}$ are predicted and assigned as $\theta_i^{m,t} = [W_i^{m,t}, b_i^{m,t}]$, as elaborated in Section 3.3 and 3.4. Input feature vectors of each modality are gradually enhanced through network blocks in their respective unimodal networks to obtain high-quality output features $f_i = \{f_i^m\}_{m=1}^M$:

$$f_i^m = N^m(x_i^m) = B^{m, \mathbf{D}_i^m} \circ \dots \circ B^{m,1}(x_i^m), \quad (1)$$

where \circ refers to the composition of two operations. Let $I_i^{m,t}$ and $I_i^{m,t+1}$ denote the input and output of the network block

$B^{m,t}$. In particular, $I_i^{m,1} = x_i^m, I_i^{m, \mathbf{D}_i^m+1} = f_i^m$. The quality enhancement by each network block $B^{m,t} : I_i^{m,t+1} = B^{m,t}(I_i^{m,t})$ can be formulated as:

$$\begin{aligned} q_i^{m,t} &= \sigma(W_i^{m,t} \cdot I_i^{m,t} + b_i^{m,t}) \\ I_i^{m,t+1} &= q_i^{m,t} \odot I_i^{m,t}. \end{aligned} \quad (2)$$

σ is the sigmoid function. $q_i^{m,t} \in \mathbb{R}^{d^m}$ is the feature-level informativeness vector of $I_i^{m,t}$ learned by $B^{m,t}$, with each element reflects the informativeness of each feature value in $I_i^{m,t}$. The quality enhancement is achieved by retaining informative features while removing redundant ones through element-wise multiplication \odot between $q_i^{m,t}$ and $I_i^{m,t}$.

The output high-quality feature vectors of all modalities $\{f_i^m\}_{m=1}^M$ are finally concatenated to provide the reliable classification result \hat{y}_i of the input sample x_i . The overall framework is trained by minimizing the classification loss \mathcal{L}^{task} , i.e., the cross-entropy loss between predictions $\{\hat{y}_i\}_{i=1}^N$ and ground-truth labels $\{y_i\}_{i=1}^N$.

3.2 Noise-free Prototype Confidence Estimation

This section introduces the Noise-free Prototype Confidence Estimation (NFCE) based on pre-optimized noise-free prototypes and classifier-free design.

Noise-Free Prototype Pre-optimization

For the dataset \mathcal{D} (M modalities and C classes), we aim to find $C \times M$ feature vectors $\omega = \{\{\omega^{c,m}\}_{c=1}^C\}_{m=1}^M$ termed noise-free prototypes. $\omega^{c,m}$ is a noise-free high confidence representative of the feature vectors of the m -th modality

from all samples under the c -th class. To learn noise-free prototypes, feature vectors of all input samples are first enhanced by modality-specific encoders. Then, the mean of all enhanced feature vectors of different modalities under different classes is calculated and yields $C \times M$ prototypes $\mu = \{\{\mu^{c,m}\}_{c=1}^C\}_{m=1}^M$. Subsequently, we eliminate noise and enhance the classification confidence of these prototypes μ , optimizing them into ω by maximizing the constraint \mathcal{L}^{rob} : $\omega = \arg \max_{\mu} \mathcal{L}^{rob}$, where \mathcal{L}^{rob} is defined as:

$$\mathcal{L}^{rob} = \frac{1}{CM^2} \sum_{c=1}^C \sum_{i=1}^M \sum_{j=1, j \neq i}^M I(\mu^{c,i}, \mu^{c,j}) + \frac{1}{CM} \sum_{m=1}^M \sum_{c=1}^C \log\left(\frac{\exp(\cos(\mu^{c,m}, \mu^{c,m}))}{\sum_{i=1}^C \exp(\cos(\mu^{c,m}, \mu^{i,m}))}\right). \quad (3)$$

$\cos(\cdot, \cdot)$ is the cosine similarity. $I(\cdot, \cdot)$ refers to mutual information between the two representations. Maximizing the first term of \mathcal{L}^{rob} removes noise and redundant features by increasing the shared information between different modalities [Federici *et al.*, 2020]. Maximizing the second term improves classification confidence by encouraging orthogonality among different classes [Huang *et al.*, 2020].

Multi-level Reliable Quality Estimation

Instead of network structures, a classifier-free design is applied that obtains noise-reliable class probability at both modality and feature levels for each input sample $x_i = \{x_i^m\}_{m=1}^M$ by contrasting it with pre-optimized noise-free prototypes ω at different levels. The modality-level class probability p_v is obtained by computing the cosine similarities between the feature vector x_i^m of each modality m and all noise-free prototypes $\omega^m = [\omega^{c,m}]_{c=1}^C$ of corresponding modality. For the feature-level probability p_f , the feature-wise absolute difference between x_i^m and ω^m is calculated:

$$p_v(x_i^m) = \text{Softmax}([\cos(x_i^m, \omega^{c,m})]_{c=1}^C) \in \mathbb{R}^C, \quad (4)$$

$$p_f(x_i^m) = \text{Softmax}([|x_i^m - \omega^{c,m}|]_{c=1}^C) \in \mathbb{R}^{d^m \times C}. \quad (5)$$

After the reliable class probability is obtained, we estimate the modality-level and feature-level quality using the true class probability [Han *et al.*, 2022] \mathcal{T} : $\delta_v(x_i^m) = \mathcal{T}(p_v(x_i^m)) \in [0, 1]$, $\delta_f(x_i^m) = \mathcal{T}(p_f(x_i^m)) \in \mathbb{R}^{d^m}$. **The detailed implementation of \mathcal{T} is given in the supplementary material.**

3.3 Global Confidence Normalized Depth

For input sample x_i , the network depth of QADM-Net is adjusted to $\{\mathbf{D}_i^m\}_{m=1}^M$ based on its modality-level qualities $\{\delta_v(x_i^m)\}_{m=1}^M$. Based on our observation in Figure 1 (a), the lower-quality modality requires a deeper network to enhance its features. Thus, a positive correlation must be maintained between $\tilde{\delta}_{v,i}^m = 1 - \delta_v(x_i^m)$ and the network depths \mathbf{D}_i^m . Instead of adjusting the depth of each modality for each sample individually, QADM-Net employs a global cross-modality depth normalization strategy. This strategy simultaneously normalizes $\{\{\tilde{\delta}_{v,i}^m\}_{m=1}^M\}_{i=1}^N$ including all modalities from all samples into a unified integer space. The normalized values

serve as the corresponding network depths of each modality for each sample $\mathbf{D} = \{\{\mathbf{D}_i^m\}_{m=1}^M\}_{i=1}^N$. On the one hand, this strategy achieves a positive correlation mapping. On the other hand, it offers a simple yet effective way to enhance the reliability of dynamic depth by normalizing the network depth distribution across modalities and mitigating the adverse effects of extreme modality samples. The calculation of this strategy can be formulated as:

$$\mathbf{D} = \{\{\mathbf{D}_i^m\}_{m=1}^M\}_{i=1}^N = \mathcal{N}_K(\{\{\tilde{\delta}_{v,i}^m\}_{m=1}^M\}_{i=1}^N). \quad (6)$$

$\mathcal{N}_K(\cdot)$ is a function that scales all the input values proportionally to integers within the range $[1, K]$, where $K \geq 1$ is an integer hyperparameter. **The analysis of K is provided in the supplementary materials.**

3.4 Layer-wise Greedy Parameter

After the depths $\{\mathbf{D}_i^m\}_{m=1}^M$ of QADM-Net for the sample x_i is determined, the Layer-wise Greedy Parameter (LGP) mechanism predicts the optimal network parameters for all network blocks. A shallow-to-deep layer-wise parameter prediction method is adopted, which can effectively handle network backbones with different depths. At each depth, the greedy strategy predicts the optimal network parameters that maximize the feature-level quality enhancement in the current layer based on how the features have been enhanced in previous depths.

Formally, At depth t ($t \in [1, \max(\mathbf{D}_i^1, \dots, \mathbf{D}_i^M)]$), we denote the network blocks of all modalities as B^t , and their inputs of all modalities as I_i^t . Since the depth of some unimodal networks might be less than t , B^t and I_i^t can be written as $B^t = \{B^{m,t} | t \in [1, \mathbf{D}_i^m]\}_{m=1}^M$ and $I_i^t = \text{Concat}(\{\hat{I}_i^{m,t}\}_{m=1}^M)$, where $\hat{I}_i^{m,t}$ equals to $I_i^{m,t}$ if $t \in [1, \mathbf{D}_i^m]$ and equals to f_i^m if $t > \mathbf{D}_i^m$. The greedy strategy jointly predicts the parameters $\{\theta_i^{m,t} | t \in [1, \mathbf{D}_i^m]\}_{m=1}^M$ corresponding to all network blocks in B^t utilizing $[I_i^1, \dots, I_i^{t-1}]$, such that the feature-level quality gain Δ_i^t at depth t is maximized:

$$\Delta_i^t = \text{mean}(\max(\delta_f(I_i^{t+1}) - \delta_f(I_i^t), \mathbf{0})), \quad (7)$$

where $I_i^{t+1} = B^t(I_i^t)$. δ_f refers to feature-level quality estimation defined in Section 3.2. $\max(\cdot, \cdot)$ is the element-wise maximization between two vectors.

In QADM-Net, we use a LSTM unit **LU** to remember the input feature vectors of previous depths and let \mathbf{LU}^{t-1} to have the memory of $[I_i^1, \dots, I_i^{t-1}]$. The input at the t -th depth I_i^t is fed into \mathbf{LU}^{t-1} to obtain modality-shared parameter information \mathbf{o}^t for all blocks of B^t . Subsequently, the shared information \mathbf{o}^t is decoded into modality-specific parameters for each block by modality-specific parameter decoders $\{\mathbf{PC}^m\}_{m=1}^M$. The calculation can be formulated as:

$$\mathbf{o}^t, \mathbf{LU}^t = \mathbf{LU}^{t-1}(I_i^t), \theta_i^{m,t} = [W_i^{m,t}, b_i^{m,t}] = \mathbf{PC}^m(\mathbf{o}^t), \text{ if } t \in [1, \mathbf{D}_i^m]. \quad (8)$$

Please refer to supplemental material for the pseudo-code of LGP. To guide LGP in predicting the optimal network parameters at each depth, in addition to maximizing Δ_i^t , a sparsity loss \mathcal{L}^s (Equation 9) is introduced to guide the prediction of

Table 1: Comparison with state-of-the-art reliable multimodal classification methods on four datasets.

| Method | Type | BRCA | | | ROSMAP | | |
|--------------------------------------|----------------|------------------|------------------|------------------|------------------|------------------|------------------|
| | | ACC | WeightedF1 | MacroF1 | ACC | F1 | AUC |
| MD [Han <i>et al.</i> , 2022] | static | 87.7±0.3 | 88.0±0.5 | 84.5±0.5 | 84.2±1.3 | 84.6±0.7 | 91.2±0.7 |
| MLCLNet [Zheng <i>et al.</i> , 2023] | static | 86.4±1.6 | 87.8±1.7 | 82.6±1.8 | 84.4±1.5 | 85.2±1.5 | 89.3±1.1 |
| DPNET [Zou <i>et al.</i> , 2023] | static | 87.8±1.0 | 88.4±1.2 | 85.2±1.2 | 85.1±1.1 | 84.8±0.7 | 91.3±0.7 |
| CALM [Zhou <i>et al.</i> , 2023] | static | 88.2±0.7 | 88.5±0.8 | 85.1±0.8 | 85.5±1.2 | 87.9±0.9 | 91.3±1.0 |
| QMF [Zhang <i>et al.</i> , 2023] | static | 87.4±0.4 | 87.7±0.5 | 84.1±0.5 | 84.6±0.9 | 84.8±0.8 | 90.5±0.8 |
| GCFANet [Zheng <i>et al.</i> , 2024] | static | 88.6±1.5 | 88.9±1.6 | 85.3±1.6 | 86.3±1.4 | 88.3±1.6 | 91.5±1.2 |
| PDF [Cao <i>et al.</i> , 2024] | static | 88.2±0.7 | 88.0±0.6 | 84.9±0.6 | 85.9±0.5 | 88.0±0.4 | 91.6±0.5 |
| DynMM [Xue and Marculescu, 2023] | dynamic | 82.3±1.7 | 82.4±1.7 | 80.1±1.2 | 81.1±1.5 | 80.2±1.6 | 80.4±1.3 |
| QADM-Net | dynamic | 93.4± 0.3 | 93.5± 0.4 | 91.5± 0.4 | 92.2± 0.4 | 92.7± 0.3 | 95.2± 0.3 |

| Method | Type | CUB | | | FOOD101 | | |
|--------------------------------------|----------------|------------------|------------------|------------------|------------------|------------------|------------------|
| | | ACC | WeightedF1 | MacroF1 | ACC | WeightedF1 | MacroF1 |
| MD [Han <i>et al.</i> , 2022] | static | 90.1±0.7 | 90.0±0.8 | 89.9±0.7 | 92.8±0.3 | 92.6±0.2 | 92.6±0.2 |
| MLCLNet [Zheng <i>et al.</i> , 2023] | static | 88.2±1.4 | 88.3±1.7 | 87.9±1.3 | 92.1±1.0 | 92.2±1.2 | 92.1±1.1 |
| DPNET [Zou <i>et al.</i> , 2023] | static | 92.1±0.9 | 91.8±0.7 | 92.2±1.1 | 93.1±1.2 | 93.0±0.7 | 92.8±0.8 |
| CALM [Zhou <i>et al.</i> , 2023] | static | 92.0±0.2 | 92.1±0.4 | 92.1±0.5 | 93.0±1.1 | 92.9±0.7 | 92.9±0.8 |
| QMF [Zhang <i>et al.</i> , 2023] | static | 89.8±0.4 | 89.7±0.5 | 89.1±0.5 | 92.7±0.5 | 92.3±0.4 | 92.4±0.4 |
| GCFANet [Zheng <i>et al.</i> , 2024] | static | 92.3±1.2 | 92.4±1.1 | 92.6±1.2 | 92.9±1.2 | 93.1±1.1 | 92.7±0.9 |
| PDF [Cao <i>et al.</i> , 2024] | static | 93.0±0.5 | 93.2±0.4 | 93.2±0.4 | 93.3±0.6 | 93.5±0.7 | 93.0±0.6 |
| DynMM [Xue and Marculescu, 2023] | dynamic | 88.3±1.5 | 88.3±1.6 | 87.7±1.5 | 89.3±1.6 | 89.4±1.7 | 88.5±1.5 |
| QADM-Net | dynamic | 97.4± 0.2 | 97.3± 0.3 | 97.4± 0.4 | 94.5± 0.3 | 94.7± 0.4 | 94.4± 0.3 |

network parameters that yield the sparsest feature informative vectors $q_i^{m,t}$ (mentioned in Equation 2), ensuring maximal removal of irrelevant and redundant information at each layer.

$$\mathcal{L}^s = \frac{1}{N} \sum_{i=1}^N \sum_{m=1}^M \sum_{t=1}^{D_i^m} \|q_i^{m,t}\|_1. \quad (9)$$

3.5 Learning

During the training stage, we first optimize the noise-free prototypes via maximizing Equation 3. Then, the overall model is trained by minimizing the loss \mathcal{L} defined as:

$$\mathcal{L} = \mathcal{L}^{task} - \Delta + \mathcal{L}^s. \quad (10)$$

\mathcal{L}^{task} is the classification loss mentioned in Section 3.1. $\Delta = \frac{1}{N} \sum_i \sum_t \Delta_i^t$ where Δ_i^t is defined in Equation 7. \mathcal{L}^s is the sparsity loss formulated in Equation 9.

4 Experiments

In this section, we conduct experiments on four real-world datasets. The main questions to be verified are highlighted here:

- Q1: How reliable is QADM-Net in classification?
- Q2: Are the two proposed dynamic mechanisms effectively improving the model’s reliability?
- Q3: Is the proposed noise-free prototype confidence estimation (NFCE) more reliable than other confidence estimation methods?
- Q4: Does QADM-Net learn informative features?
- Q5: How is QADM-Net’s computation efficiency?

4.1 Experimental Settings

Datasets. Experiments are conducted on four commonly used multimodal datasets in previous methods [Han *et al.*, 2020; Geng *et al.*, 2021; Han *et al.*, 2022; Zhang *et al.*, 2023; Zheng *et al.*, 2023; Zhou *et al.*, 2023; Cao *et al.*, 2024]. (1) **BRCA** is a dataset for classifying breast invasive carcinoma into 5 PAM50 subtypes, containing 875 samples with features from three modalities: mRNA expression, DNA methylation, and miRNA expression. It is available from The Cancer Genome Atlas (TCGA).¹ (2) **ROSMAP** contains samples from Alzheimer’s patients (182 samples) and normal control subjects (169 samples) including same modalities as **BRCA**. [A Bennett *et al.*, 2012; De Jager *et al.*, 2018] (3) **CUB** is an image-text dataset with 11,788 samples comprising 200 categories of birds. [Wah *et al.*, 2011] (4) **UPMC FOOD101** comprises 90,704 food images from 101 categories and corresponding textual descriptions [Wang *et al.*, 2015].

Compared methods. To demonstrate the improvement in multimodal classification reliability achieved by the proposed QADM-Net, several representative methods in this field are introduced, including multimodal dynamics (**MD**) [Han *et al.*, 2022], multi-level confidence learning (**MLCLNet**) [Zheng *et al.*, 2023], dynamic poly-attention network (**DPNET**) [Zou *et al.*, 2023], enhanced encoding and confidence evaluating framework (**CALM**) [Zhou *et al.*, 2023], quality-aware multimodal fusion (**QMF**) [Zhang *et al.*, 2023], multi-omics data classification network via global and cross-modal feature aggregation (**GCFANet**) [Zheng *et*

¹<https://www.cancer.gov/aboutnci/organization/ccg/research/structuralgenomics/tcga>

et al., 2024], and predictive dynamic fusion (PDF) [Cao *et al.*, 2024]. To demonstrate the advantages of our method over other multimodal dynamic neural network, **DynMM** [Xue and Marculescu, 2023] is also included in the experiments. Other dynamic neural networks are excluded from the experiments as they are not applicable to multimodal scenarios.

Evaluation metrics. For multi-class classification tasks, three metrics, including accuracy (ACC), average F1 score weighted by support (WeightedF1), and macro-averaged F1 score (MacroF1), are employed to evaluate the performance of different methods. For binary classification tasks, ACC, F1 score (F1), and area under the receiver operating characteristic curve (AUC) of different methods are compared.

Implementation details. Noise is added to simulate low-quality data in the experiments, with σ representing the noise intensity. We run experiments 20 times to report the mean and standard deviation, following previous work [Han *et al.*, 2022]. The Adam optimizer and the step learning rate scheduler with an initial learning rate of $1e-4$ are employed in the training. **More implementation details, including the noise-adding process, are provided in the supplementary material.**

4.2 Experimental Results

Classification Performance (Q1)

Following previous works [Han *et al.*, 2020; Ma *et al.*, 2021; Zhang *et al.*, 2023; Zhou *et al.*, 2023], we compare the classification performance of different methods under noise-free (Table 1) and Gaussian noise-added (Figure 3) settings. The results demonstrate that: (1) QADM-Net with network dynamics achieves more promising and stable classification performance under different noise intensities compared to its static counterparts. (2) QADM-Net outperforms **DynMM**. The possible reasons include QADM-Net’s reliable confidence estimation for samples, more robust dynamic depth under the global cross-modality depth normalization, and its capability for dynamic network parameters.

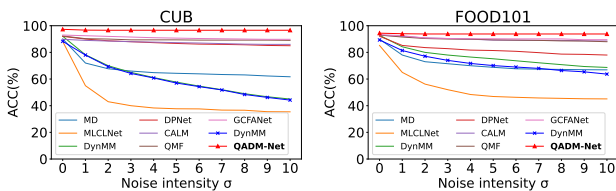


Figure 3: Comparison of classification accuracy of different models under Gaussian noise with different intensities σ .

Ablation study (Q2)

We conduct ablation studies on all four datasets to demonstrate the effectiveness of the Global Confidence Normalized Depth (GCND) and Layer-wise Greedy Parameter (LGP) mechanisms in enhancing the reliability of QADM-Net. To this end, two degraded model versions, “W/O GCND” and “W/O LGP”, are introduced. In “W/O GCND”, the depth of each unimodal model is fixed to the hyperparameter K . In

Table 2: Ablation study on four datasets to demonstrate the effectiveness of LGP, where the best results are in bold.

| Dataset | Method | $\sigma = 0$ | $\sigma = 5$ | $\sigma = 10$ |
|---------|-----------------|--------------|--------------|---------------|
| BRCA | W/O LGP | 86.2 | 83.4 | 80.2 |
| | QADM-Net | 93.4 | 92.4 | 91.5 |
| ROSMAP | W/O LGP | 85.4 | 82.6 | 80.4 |
| | QADM-Net | 92.2 | 91.6 | 90.8 |
| CUB | W/O LGP | 90.3 | 86.2 | 83.6 |
| | QADM-Net | 97.4 | 96.7 | 95.5 |
| FOOD101 | W/O LGP | 90.2 | 87.7 | 85.1 |
| | QADM-Net | 94.5 | 93.8 | 93.0 |

“W/O LGP”, the parameters of all network blocks are determined during training instead of dynamically predicted during inference. **(i) Effectiveness of GCND.** Figure 4 shows the classification accuracy of “W/O GCND” and QADM-Net on four datasets. When $K = 1$, the two network structures are identical, resulting in the same accuracy. When $K \geq 2$, QADM-Net’s unimodal networks can dynamically adjust their depth between 1 and K . In contrast, “W/O GCND” maintains a fixed depth of K , which becomes too deep for a significant portion of easy samples in the dataset, causing overfitting and a notable performance drop. As K increases, the issues with “W/O GCND” become more severe, resulting in a continuous decline in accuracy. **(ii) Effectiveness of LGP.** Table 2 compares the classification accuracy of “W/O LGP” and QADM-Net on four datasets under different noise intensities. QADM-Net outperforms “W/O LGP” across different noise levels, and its performance degradation as noise intensity increases is significantly less severe than “W/O LGP”. This demonstrates that LGP contributes to both higher classification performance and improved robustness.

We have conducted extensive experiments to show **the sample-adaptiveness of QADM-Net**, the robustness of GCND to extreme samples, the enhancements in modality and feature quality across layers by GCND and LGP, and so on. **Due to space limitations, more experimental results are presented in the supplementary materials.**

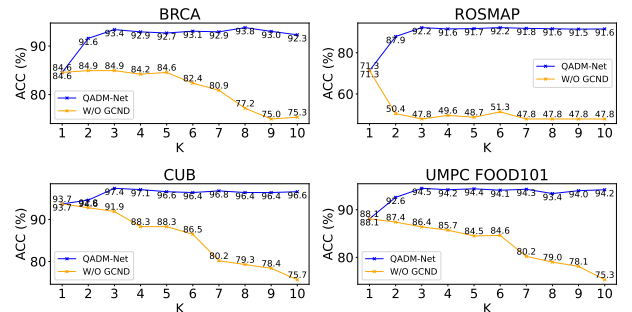


Figure 4: Ablation study to demonstrate the effectiveness of GCND.

Reliability of the Proposed NFCE (Q3)

We conduct experiments on commonly used traditional confidence estimation methods, including MCP, TCP [Han *et al.*,

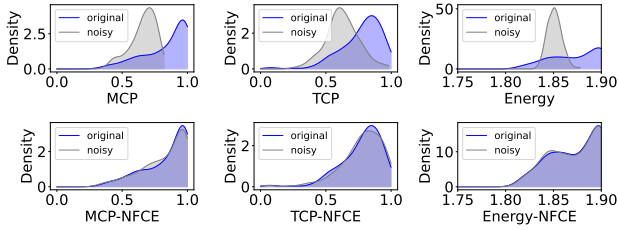


Figure 5: Comparison of the sensitivity of some commonly used traditional confidence assessment methods and their “-NFCE” counterparts to training noise on the FOOD101 dataset.

Table 3: Results of QADM-Net on the FOOD101 dataset using different confidence estimation methods.

| Method | $\sigma = 0$ | $\sigma = 1$ | $\sigma = 5$ |
|-----------------|--------------|--------------|--------------|
| QADM-Net (Cls) | 93.5 | 91.7 | 90.4 |
| QADM-Net (NFCE) | 94.5 | 94.0 | 93.8 |

2022], and Energy [Liu *et al.*, 2020], all of which assess confidence based on class probabilities obtained by network or classifier. To demonstrate that the proposed noise-free prototype confidence estimation can enhance the reliability of these methods, we replaced their class probability computing approach with the method described in Equation 4, resulting in “MCP-NFCE”, “TCP-NFCE”, and “Energy-NFCE”, respectively. Each method is trained separately on the original and noisy training set with Gaussian noise ($\sigma = 5$). Figure 5 reports the confidence estimation of the same clean testing samples provided by two trained versions of each method. The testing results obtained by the same method after training on original and noisy data are expected to be nearly identical since the confidence evaluation is performed on the same test samples. However, the results of the three traditional methods exhibit shifts. Notably, the testing confidence corresponding to the noisy training set is significantly lower than that of the original. The reason is that the classifiers or network structures in these methods overfit the noise distribution, resulting in reduced classification confidence for clean test samples. In contrast, the three “-NFCE” counterparts maintain stable testing confidence for different training noises. Thanks to the noise-free prototypes and the classifier-free design, the confidence of samples can be evaluated more reliably. Furthermore, we substitute the method of Equation 4 in QADM-Net with classifier and yield “QADM-Net (Cls)”. Table 3 compares the classification accuracy of “QADM-Net (Cls)” and original QADM-Net with NFCE under different noise inten-

Table 4: Top 5 informative biomarkers that QADM-Net learned from different modalities on BRCA dataset.

| Modality | Top 5 informative biomarkers |
|----------|---|
| DNA | ZNF671, KRTAP3-1, ZCCHC8, AGR2, MYT1 |
| mRNA | KLK8, MIA, PTX3, SOX11, KRT6B |
| miRNA | mir-378, mir-190b, mir-934, mir-21, mir-23b |

Table 5: Comparison of ACC and FLOPs per sample of different methods on the FOOD101 dataset, where * are the results under Gaussian noise with $\sigma = 5$.

| Method | GCFANet | PDF | DynMM | QADM-Net |
|------------|-------------|-------------|---------------|--------------------|
| ACC (%) | 92.9 | 93.3 | 89.3 | 94.5 |
| FLOPs (M) | 9.22 | 3.53 | 3.71 | 3.82 |
| ACC* (%) | 89.4 (-3.5) | 90.1 (-3.2) | 70.1 (-19.2) | 93.8 (-0.7) |
| FLOPs* (M) | 9.22 (+0) | 3.53 (+0) | 10.82 (+7.11) | 8.94 (+5.12) |

sities. The results indicate that NFCE provides QADM-Net with greater reliability than classifier-based.

We also conducted experiments showing that noise-free prototypes effectively eliminate data noise and that NFCE achieves multi-level quality estimation. **Results are provided in the supplementary material.**

Informative features that QADM-Net learns (Q4)

We further demonstrate the reliability of QADM-Net by analyzing the informative features it retains following previous works [Han *et al.*, 2022; Zou *et al.*, 2023]. Table 4 shows the top 5 informative biomarkers of the three modalities on the BRCA dataset retained by the feature informativeness masks $q_i^{m,t}$ (Equation 2) in QADM-Net, which align with the findings of existing biomedical research. For example, Low expression of ZNF671 [Zhang *et al.*, 2019], miR-378 [Arabkari *et al.*, 2023] are both associated with poor prognosis in breast cancer. KLK8 is an independent indicator of prognosis in breast cancer patients [Michaelidou *et al.*, 2015].

Computation Effectiveness of QADM-Net (Q5)

Although computational efficiency is not the design motivation or novelty of QADM-Net, it maintains the high computational efficiency characteristic of dynamic networks while ensuring model robustness. Table 5 compares the classification accuracy and corresponding FLOPs of QADM-Net with some SOTA reliable multimodal classification methods and the multimodal dynamic neural network **DynMM** on both clean and noisy datasets. QADM-Net achieves most stable and promising results with only a 5.12M increase in FLOPs (less than **DynMM** and still lower than **GCFANet** after the increase), demonstrating its computation efficiency while ensuring model reliability. **Further comparison of the parameter amounts can be found in the supplementary material.**

5 Conclusions

This work proposes a novel multi-level quality-adaptive dynamic multimodal network (QADM-Net) for reliable multimodal classification. On the one hand, QADM-Net adopts a reliable multi-level quality estimation method NFCE based on noise-free prototypes and classifier-free design. On the other hand, QADM-Net proposed two mechanisms termed GCND and LGP to achieve sample-adaptive network depth and parameters based on modality and feature level quality, significantly promoting inference reliability. Extensive experiments show the superiority of QADM-Net in classification performance compared to state-of-the-art reliable classification methods and demonstrate the strong adaptability of QADM-Net to data with diverse quality.

References

- [A Bennett *et al.*, 2012] David A Bennett, Julie A Schneider, Zoe Arvanitakis, and Robert S Wilson. Overview and findings from the religious orders study. *Current Alzheimer Research*, 9(6):628–645, 2012.
- [Arabkari *et al.*, 2023] Vahid Arabkari, David Barua, Muhammad Mosaraf Hossain, Mark Webber, Terry Smith, Ananya Gupta, and Sanjeev Gupta. mirna-378 is downregulated by xbp1 and inhibits growth and migration of luminal breast cancer cells. *International Journal of Molecular Sciences*, 25(1):186, 2023.
- [Cao *et al.*, 2024] Bing Cao, Yanan Xia, Yi Ding, Changqing Zhang, and Qinghua Hu. Predictive dynamic fusion. In Ruslan Salakhutdinov, Zico Kolter, Katherine Heller, Adrian Weller, Nuria Oliver, Jonathan Scarlett, and Felix Berkenkamp, editors, *Proceedings of the 41st International Conference on Machine Learning*, volume 235 of *Proceedings of Machine Learning Research*, pages 5608–5628. PMLR, 21–27 Jul 2024.
- [De Jager *et al.*, 2018] PL De Jager, Y Ma, C McCabe, J Xu, BN Vardarajan, D Felsky, HU Klein, CC White, MA Peters, B Lodgson, et al. A multi-omic atlas of the human frontal cortex for aging and alzheimer’s disease research. *sci data* 5: 180142, 2018.
- [Dou *et al.*, 2022] Zi-Yi Dou, Yichong Xu, Zhe Gan, Jianfeng Wang, Shuohang Wang, Lijuan Wang, Chenguang Zhu, Pengchuan Zhang, Lu Yuan, Nanyun Peng, et al. An empirical study of training end-to-end vision-and-language transformers. In *Proceedings of the IEEE/CVF Conference on Computer Vision and Pattern Recognition*, pages 18166–18176, 2022.
- [Elizalde *et al.*, 2023] Benjamin Elizalde, Soham Deshmukh, Mahmoud Al Ismail, and Huaming Wang. Clap learning audio concepts from natural language supervision. In *ICASSP 2023-2023 IEEE International Conference on Acoustics, Speech and Signal Processing (ICASSP)*, pages 1–5. IEEE, 2023.
- [Federici *et al.*, 2020] Marco Federici, Anjan Dutta, Patrick Forré, Nate Kushman, and Zeynep Akata. Learning robust representations via multi-view information bottleneck. *arXiv preprint arXiv:2002.07017*, 2020.
- [Feng *et al.*, 2018] Di Feng, Lars Rosenbaum, and Klaus Dietmayer. Towards safe autonomous driving: Capture uncertainty in the deep neural network for lidar 3d vehicle detection. In *2018 21st international conference on intelligent transportation systems (ITSC)*, pages 3266–3273. IEEE, 2018.
- [Geng *et al.*, 2021] Yu Geng, Zongbo Han, Changqing Zhang, and Qinghua Hu. Uncertainty-aware multi-view representation learning. In *Proceedings of the AAAI Conference on Artificial Intelligence*, volume 35, pages 7545–7553, 2021.
- [Han *et al.*, 2020] Zongbo Han, Changqing Zhang, Huazhu Fu, and Joey Tianyi Zhou. Trusted multi-view classification. In *International Conference on Learning Representations*, 2020.
- [Han *et al.*, 2021] Yizeng Han, Gao Huang, Shiji Song, Le Yang, Honghui Wang, and Yulin Wang. Dynamic neural networks: A survey. *IEEE Transactions on Pattern Analysis and Machine Intelligence*, 44(11):7436–7456, 2021.
- [Han *et al.*, 2022] Zongbo Han, Fan Yang, Junzhou Huang, Changqing Zhang, and Jianhua Yao. Multimodal dynamics: Dynamical fusion for trustworthy multimodal classification. In *Proceedings of the IEEE/CVF conference on computer vision and pattern recognition*, pages 20707–20717, 2022.
- [Hua *et al.*, 2019] Weizhe Hua, Yuan Zhou, Christopher M De Sa, Zhiru Zhang, and G Edward Suh. Channel gating neural networks. *Advances in Neural Information Processing Systems*, 32, 2019.
- [Huang *et al.*, 2017] Gao Huang, Danlu Chen, Tianhong Li, Felix Wu, Laurens Van Der Maaten, and Kilian Q Weinberger. Multi-scale dense networks for resource efficient image classification. *arXiv preprint arXiv:1703.09844*, 2017.
- [Huang *et al.*, 2020] Jiabo Huang, Shaogang Gong, and Xiaotian Zhu. Deep semantic clustering by partition confidence maximisation. In *Proceedings of the IEEE/CVF conference on computer vision and pattern recognition*, pages 8849–8858, 2020.
- [Li *et al.*, 2022] Manling Li, Ruochen Xu, Shuohang Wang, Luowei Zhou, Xudong Lin, Chenguang Zhu, Michael Zeng, Heng Ji, and Shih-Fu Chang. Clip-event: Connecting text and images with event structures. In *Proceedings of the IEEE/CVF conference on computer vision and pattern recognition*, pages 16420–16429, 2022.
- [Lin *et al.*, 2023] Zhihao Lin, Yongtao Wang, Jinhe Zhang, and Xiaojie Chu. Dynamicdet: A unified dynamic architecture for object detection. In *Proceedings of the IEEE/CVF Conference on Computer Vision and Pattern Recognition*, pages 6282–6291, 2023.
- [Liu *et al.*, 2020] Weitang Liu, Xiaoyun Wang, John Owens, and Yixuan Li. Energy-based out-of-distribution detection. *Advances in neural information processing systems*, 33:21464–21475, 2020.
- [Ma *et al.*, 2021] Huan Ma, Zongbo Han, Changqing Zhang, Huazhu Fu, Joey Tianyi Zhou, and Qinghua Hu. Trustworthy multimodal regression with mixture of normal-inverse gamma distributions. *Advances in Neural Information Processing Systems*, 34:6881–6893, 2021.
- [Michaelidou *et al.*, 2015] Kleita Michaelidou, Alexandros Ardavanis, and Andreas Scorilas. Clinical relevance of the deregulated kallikrein-related peptidase 8 mrna expression in breast cancer: a novel independent indicator of disease-free survival. *Breast cancer research and treatment*, 152:323–336, 2015.
- [Nair *et al.*, 2020] Tanya Nair, Doina Precup, Douglas L Arnold, and Tal Arbel. Exploring uncertainty measures in deep networks for multiple sclerosis lesion detection and segmentation. *Medical image analysis*, 59:101557, 2020.

- [Su *et al.*, 2019] Hang Su, Varun Jampani, Deqing Sun, Orazio Gallo, Erik Learned-Miller, and Jan Kautz. Pixel-adaptive convolutional neural networks. In *Proceedings of the IEEE/CVF Conference on Computer Vision and Pattern Recognition*, pages 11166–11175, 2019.
- [Sun *et al.*, 2022] Hao Sun, Hongyi Wang, Jiaqing Liu, Yen-Wei Chen, and Lanfen Lin. Cubemlp: An mlp-based model for multimodal sentiment analysis and depression estimation. In *Proceedings of the 30th ACM international conference on multimedia*, pages 3722–3729, 2022.
- [Tellamekala *et al.*, 2023] Mani Kumar Tellamekala, Shahin Amiriparian, Björn W Schuller, Elisabeth André, Timo Giesbrecht, and Michel Valstar. Cold fusion: Calibrated and ordinal latent distribution fusion for uncertainty-aware multimodal emotion recognition. *IEEE Transactions on Pattern Analysis and Machine Intelligence*, 2023.
- [Veit and Belongie, 2018] Andreas Veit and Serge Belongie. Convolutional networks with adaptive inference graphs. In *Proceedings of the European conference on computer vision (ECCV)*, pages 3–18, 2018.
- [Wah *et al.*, 2011] Catherine Wah, Steve Branson, Peter Welinder, Pietro Perona, and Serge Belongie. The caltech-ucsd birds-200-2011 dataset. 2011.
- [Wang *et al.*, 2015] Xin Wang, Devinder Kumar, Nicolas Thome, Matthieu Cord, and Frederic Precioso. Recipe recognition with large multimodal food dataset. In *2015 IEEE International Conference on Multimedia & Expo Workshops (ICMEW)*, pages 1–6. IEEE, 2015.
- [Xue and Marculescu, 2023] Zihui Xue and Radu Marculescu. Dynamic multimodal fusion. In *Proceedings of the IEEE/CVF Conference on Computer Vision and Pattern Recognition*, pages 2575–2584, 2023.
- [Zhang *et al.*, 2019] Jian Zhang, Ziqi Zheng, Jieling Zheng, Tao Xie, Yunhong Tian, Rong Li, Baiyao Wang, Jie Lin, Anan Xu, Xiaoting Huang, et al. Epigenetic-mediated downregulation of zinc finger protein 671 (znf671) predicts poor prognosis in multiple solid tumors. *Frontiers in Oncology*, 9:342, 2019.
- [Zhang *et al.*, 2023] Qingyang Zhang, Haitao Wu, Changqing Zhang, Qinghua Hu, Huazhu Fu, Joey Tianyi Zhou, and Xi Peng. Provable dynamic fusion for low-quality multimodal data. In *International conference on machine learning*, pages 41753–41769. PMLR, 2023.
- [Zhang *et al.*, 2024] Qingyang Zhang, Yake Wei, Zongbo Han, Huazhu Fu, Xi Peng, Cheng Deng, Qinghua Hu, Cai Xu, Jie Wen, Di Hu, et al. Multimodal fusion on low-quality data: A comprehensive survey. *arXiv preprint arXiv:2404.18947*, 2024.
- [Zheng *et al.*, 2023] Xiao Zheng, Chang Tang, Zhiguo Wan, Chengyu Hu, and Wei Zhang. Multi-level confidence learning for trustworthy multimodal classification. In *Proceedings of the AAAI Conference on Artificial Intelligence*, volume 37, pages 11381–11389, 2023.
- [Zheng *et al.*, 2024] Xiao Zheng, Minhui Wang, Kai Huang, and En Zhu. Global and cross-modal feature aggregation for multi-omics data classification and application on drug response prediction. *Information Fusion*, 102:102077, 2024.
- [Zhou *et al.*, 2023] Hai Zhou, Zhe Xue, Ying Liu, Boang Li, Junping Du, Meiyu Liang, and Yuankai Qi. Calm: An enhanced encoding and confidence evaluating framework for trustworthy multi-view learning. In *Proceedings of the 31st ACM International Conference on Multimedia*, pages 3108–3116, 2023.
- [Zou *et al.*, 2023] Xin Zou, Chang Tang, Xiao Zheng, Zhenglai Li, Xiao He, Shan An, and Xinwang Liu. Dpnet: Dynamic poly-attention network for trustworthy multimodal classification. In *Proceedings of the 31st ACM International Conference on Multimedia*, pages 3550–3559, 2023.